

UNCLASSIFIED

Defense Technical Information Center  
Compilation Part Notice

ADP013694

TITLE: Instability of the Shear Layer Separating from a Circular Cylinder

DISTRIBUTION: Approved for public release, distribution unlimited

This paper is part of the following report:

TITLE: DNS/LES Progress and Challenges. Proceedings of the Third  
AFOSR International Conference on DNS/LES

To order the complete compilation report, use: ADA412801

The component part is provided here to allow users access to individually authored sections of proceedings, annals, symposia, etc. However, the component should be considered within the context of the overall compilation report and not as a stand-alone technical report.

The following component part numbers comprise the compilation report:

ADP013620 thru ADP013707

UNCLASSIFIED

# INSTABILITY OF THE SHEAR LAYER SEPARATING FROM A CIRCULAR CYLINDER

JINSUNG KIM AND HAECHAEON CHOI

*School of Mechanical and Aerospace Engineering  
Seoul National University, Seoul 151-742, Korea*

**Abstract.** The instability of the shear layer separating from a circular cylinder has been investigated using large eddy simulation at two different Reynolds numbers of 1600 and 3900 based on the free-stream velocity and cylinder diameter. Two distinct types of the shear layer instability are found in this study: one is a completely three-dimensional type and the other is a quasi-two-dimensional type. The instability of three-dimensional type is generated by a strong counter-rotating streamwise vortex pair underneath the separating shear layer and thus occurs locally in the spanwise direction. On the other hand, the instability of quasi-two-dimensional type is associated with the breakdown of the Karman vortex shedding process and thus occurs globally across the cross-stream direction as well as the spanwise direction, resulting in the in-phase shear layer instability. It is also conjectured that at high Reynolds number, the instability of quasi-two-dimensional type should be more frequent than the instability of three-dimensional type.

## 1. Introduction

The separated shear layer is one of the important flow characteristics in the flow around a circular cylinder. Bloor (1964) is the one who first performed the systematic measurement of the shear layer separating from a circular cylinder. She used a hot-wire probe to measure the frequency of transition wave in the shear layer. She concluded that the transition wave exists for  $Re > Re_{crit} = 1300$  and suggested that the shear-layer frequency normalized by the primary vortex-shedding frequency ( $f_{SL}/f_K$ ) scales with  $Re^{1/2}$ , where  $Re = u_\infty d/\nu$ ,  $u_\infty$  is the free-stream velocity,  $d$  is the cylinder diameter, and  $\nu$  is the kinematic viscosity. After Bloor's (1964) experiment, several other researchers have investigated the shear-layer instability. Wei

& Smith (1986) found that the transition wave of Bloor (1964) is an identical phenomenon to the roll-up of small-scale secondary vortices in the shear layer. They also reported that the normalized shear-layer frequency varies as  $Re^{0.77}$  from hot-wire measurements and as  $Re^{0.87}$  from flow visualization, which are contrary to the 0.5 power law of Bloor (1964). Unal & Rockwell (1988a) reported that the instability could not be perceived for  $Re < 1900$  from both the hot-film measurement and flow visualization and pointed out the influence of background disturbances to  $Re_{crit}$ . Recently, Prasad & Williamson (1996, 1997) showed that a power law of the form  $Re^{0.67}$  accurately represents the  $Re$ -variation of  $f_{SL}/f_K$ . The effect of the spanwise end condition on  $Re_{crit}$  is also examined by Prasad & Williamson (1996, 1997). They reported that  $Re_{crit} \approx 1200$  for parallel shedding and  $Re_{crit} \approx 2600$  for oblique shedding.

In this study, we investigate the shear-layer instability around a circular cylinder at two different Reynolds numbers of  $Re = 1600$  and  $3900$ , which are higher than  $Re_{crit}$  suggested by Prasad & Williamson (1996, 1997), using large eddy simulation.

## 2. Numerical method

Large eddy simulations are performed with the dynamic subgrid-scale model (Germano *et al.* 1991; Lilly 1992) in generalized coordinates. The time integration method is based on a fully implicit, fractional step method (Choi *et al.* 1992; Choi & Moin 1994). All terms including cross-derivative diffusion terms are advanced with the Crank-Nicolson method in time and are resolved with the second-order central-difference scheme in space. The computational domain is  $-19d \leq x \leq 17d$ ,  $-25d \leq y \leq 25d$ , where  $(x = 0, y = 0)$  corresponds to the center location of the cylinder. The spanwise length of the cylinder is chosen to be  $\pi d$ . This spanwise domain length was used by other investigators (Mittal & Moin 1997; Kravchenko & Moin 1998). A C-type mesh with  $673 \times 160 \times 64$  grid points is used and the computational time step used is  $\Delta t u_\infty/d = 0.0095$ . With this mesh and computational time step, the maximum CFL number is about 3.0 for  $Re=1600$  and about 3.4 for  $Re=3900$ . The computations are performed using 42 processor elements in CRAY T3E. The computational cost is about 8 hours per vortex shedding period per processor element.

## 3. Result

We observe the instability of the shear layer from both vortical structures and velocity time traces. Figure 1 shows the time traces of the streamwise velocity at  $x/d = 1.0$  and  $y/d = 0.8$  at a few different spanwise locations at  $Re=1600$ . The same  $(x, y)$  location was also selected by Prasad &

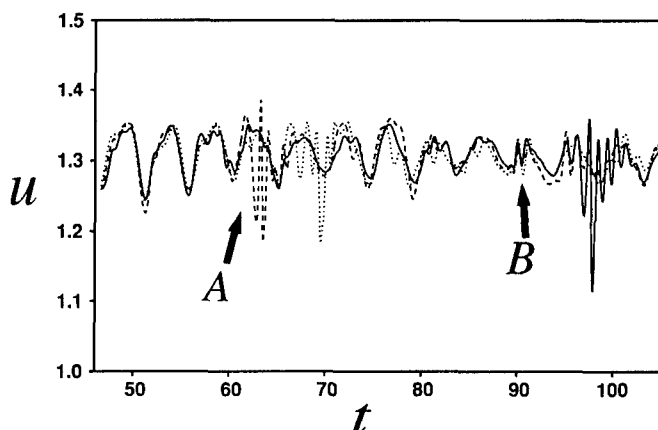


Figure 1. Time traces of the streamwise velocity at  $x/d = 1.0$  and  $y/d = 0.8$  ( $Re=1600$ ).

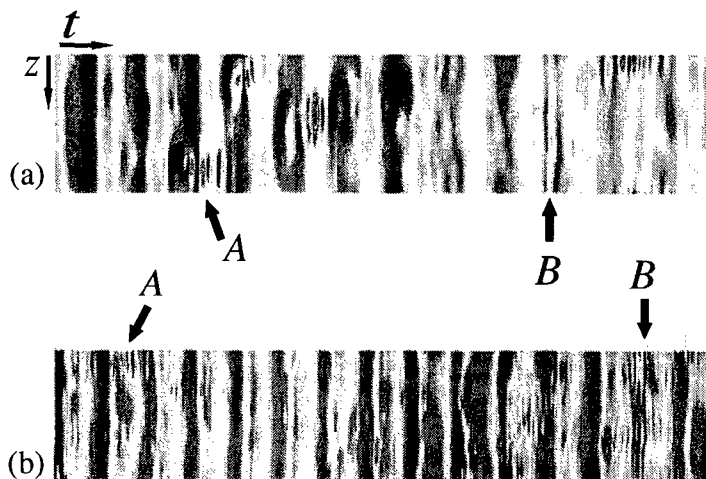


Figure 2. Contours of the streamwise velocity fluctuations at  $x/d = 1.0$  and  $y/d = 0.8$  in the  $t-z$  plane: (a)  $Re=1600$ ; (b)  $Re=3900$ .

Williamson (1996, 1997) to observe the shear-layer instability. It is clearly seen from figure 1 that the shear-layer instability (packet of intermittent high frequency velocity fluctuations) occurs. The time traces at  $Re=3900$  are similar to those shown in figure 1 (not shown here). It is interesting to note that there exist two distinct types of the shear-layer instability: one is denoted by 'A', whereas the other is denoted by 'B' (figure 1). In the case of type 'A' instability, the intermittent velocity fluctuations exist locally in the spanwise direction. That is, the shear-layer instability of this type is a completely three-dimensional phenomenon. So we call this type

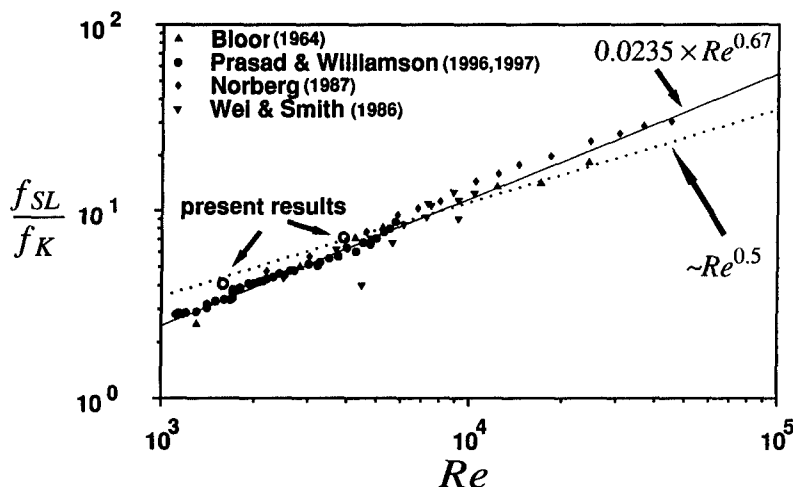


Figure 3. Variation of the normalized shear-layer frequency with respect to the Reynolds number ( $f_{SL}$ : shear-layer frequency,  $f_K$ : natural-shedding frequency).

'A' instability as a 3-D instability. For the type 'B' instability, the intermittent velocity fluctuations occur simultaneously at all spanwise positions and thus we call this type as a quasi-2-D instability.

The difference between the 3-D and quasi-2-D instabilities can be seen more clearly from figures 2(a) and 2(b). All the data from every other grid points in the spanwise direction are included in figures 2(a) and 2(b) where the horizontal direction is the time axis and the vertical direction is the spanwise direction. One can see that the 3-D instability signals form an 'island' in the  $t-z$  plane, whereas the quasi-2-D instability appears as vertical lines. Figure 2 also shows that the packets of shear-layer velocity fluctuations occur more frequently at  $Re = 3900$  than at  $Re = 1600$ , which agrees with the finding of Prasad & Williamson (1997) about the Reynolds-number dependence.

The frequency of the shear-layer instability is calculated from the stream-wise velocity time trace. The normalized shear-layer frequencies are shown in figure 3, together with the results of other experiments (from Prasad & Williamson 1996, 1997). Two lines in figure 3 are  $Re^{0.5}$  and  $Re^{0.67}$  variations suggested by Bloor (1964) and Prasad & Williamson (1996, 1997), respectively. The shear-layer frequencies of the present study are a little higher than other results, but the difference is acceptable considering the discrepancy between the experiments.

Figure 4 shows the vortical structures near the cylinder at  $Re = 1600$ . The vortex-identification method by Jeong & Hussain (1995) is used to visualize the three-dimensional vortical structures, where  $\lambda_2$  is the second

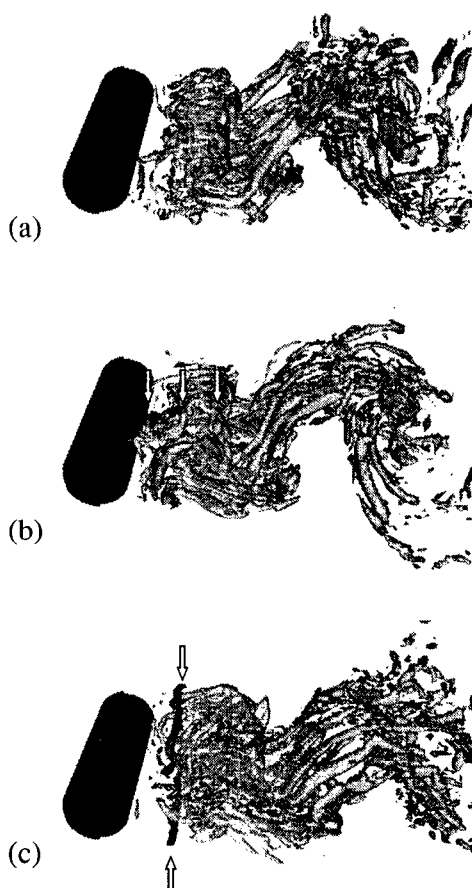


Figure 4. Vortical structures at  $Re = 1600$  (iso-surfaces of  $\lambda_2 = -10$ ): (a) no shear layer vortex; (b) 3-D type shear-layer vortices; (c) quasi-2-D type shear-layer vortices.

largest eigenvalue of  $S^2 + \Omega^2$  ( $S$  and  $\Omega$  are the strain rate and rotation rate tensors, respectively). Figure 4(a) is instantaneous vortical structures when there is no shear-layer vortex. On the other hand, figures 4(b) and 4(c) show the spanwise roll-up vortices for the cases of 3-D and quasi-2-D instabilities, respectively, from which one can easily figure out the difference between two instabilities. In the case of quasi-2-D type, roll-up of shear-layer vortex occurs throughout the span, whereas the roll-up vortices exist locally in the spanwise direction in the case of 3-D type. Another important difference between the 3-D and quasi-2-D type roll-up vortices is the correlation between the upper and lower shear-layer vortices. The



Figure 5. 3-D type shear-layer vortices and streamwise vortices: (a) iso-surface of  $\lambda_2 = -10$ ; (b) iso-surfaces of  $\omega_x = +10$  (light color) and  $\omega_x = -10$  (dark color).

quasi-2-D vortices appear in-phase in the upper and lower shear layers of the cylinder, but for the 3-D type there is no correlation between the upper and lower shear layers. Flow visualization of Prasad & Williamson (1997) shows the in-phase behavior of the shear-layer instability that is analogous to the quasi-2-D instability of the present study. Wei & Smith (1986) used the hydrogen-bubble flow-visualization method and showed several side and top views. Some of the top views are similar to our 3-D instability, although their side views show the configuration similar to the in-phase roll-up. At  $Re = 3900$ , the shear-layer characteristics are similar to those at  $Re = 1600$ , although the length scale of vortical structures is smaller at  $Re = 3900$ .

Figure 5 shows an instantaneous flow structure together with the iso-surfaces of the streamwise vorticity, when the 3-D type vortex roll-up occurs. It is clearly seen that a strong streamwise vortex pair exists underneath the shear layer roll-up vortices of 3-D type. That is, the 3-D instability is locally stimulated by strong streamwise vortices underneath the separated shear layer.

The quasi-2-D instability is closely related to the natural vortex-shedding process. When the natural vortex-shedding process is weakened or disor-

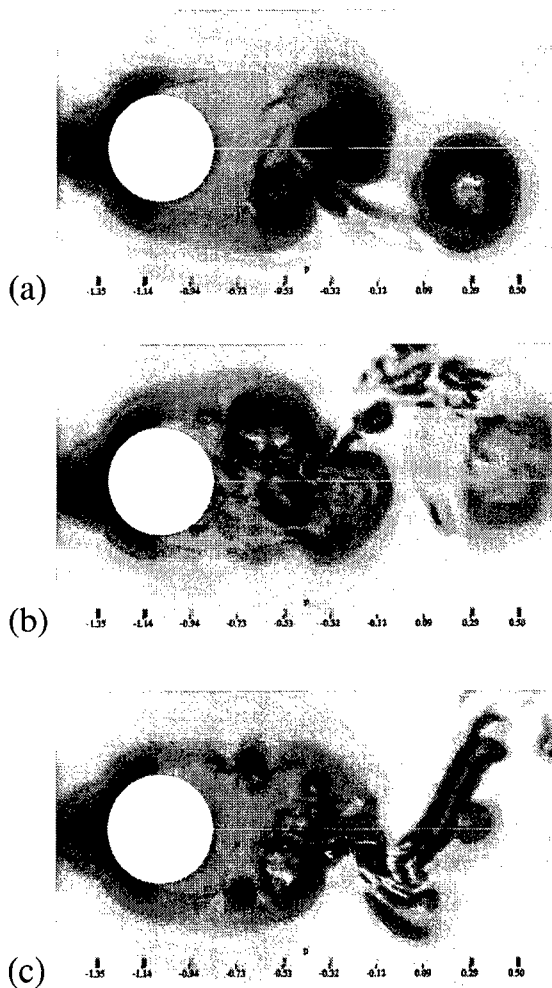


Figure 6. Contours of the instantaneous pressure in an  $(x-y)$  plane: (a) regular shedding; (b) corrupted vortex core; (c) quasi-2-D vortex roll-up.

dered due to turbulence, the shear layers both in the upper and lower sides of the cylinder evolve further downstream and thus both the shear layers become thinner and nearly symmetric with respect to each other. When this happens, the quasi-2-D vortex appears in the shear layer and the shear-layer instability occurs at the upper and lower sides simultaneously (in-phase). This process is shown in figure 6. Figure 6(a) shows the instantaneous pressure contours in the case of regular vortex shedding, whereas figure 6(b) shows those in the case of breakdown of the Karman vortex shedding process, resulting in the in-phase roll-up of quasi-2-D shear-layer vortices as shown in figure 6(c).

#### 4. Summary

In summary, two distinct types of the shear-layer instability are found using large eddy simulation for flow over a circular cylinder at  $Re = 1600$  and  $Re = 3900$ . One is the 3-D type instability that is generated locally by a strong counter-rotating streamwise vortex pair. The other instability is the quasi-2-D type instability, characterized by vortex roll-up occurred simultaneously along the spanwise direction as well as at upper and lower sides of the cylinder. This instability is initiated from disorder of the Karman vortex shedding process. It is conjectured that when the Reynolds number is higher than the present ones, the shear-layer thickness should become smaller and the quasi-2-D vortex roll-up is more likely to occur than the 3-D vortex roll-up.

This work is supported by the Creative Research Initiatives of the Korean Ministry of Science and Technology.

#### References

- BLOOR, M. S. 1964 The transition to turbulence in the wake of a circular cylinder. *J. Fluid Mech.* **19**, 290–304.
- CHOI, H., MOIN, P. & KIM, J. 1992 Turbulent drag reduction: Studies of feedback control and flow over riblets. *Report No. TF-55*. Department of Mechanical Engineering, Stanford University
- CHOI, H. & MOIN, P. 1994 Effects of the computational time step on numerical solutions of turbulent flow. *J. Comput. Phys.* **113**, 1–4.
- GERMANO, M., PIOMELLI, U., MOIN, P. & CABOT, W. 1991 A dynamic subgrid-scale eddy viscosity model. *Phys. Fluids*, **3**, 1760–1765.
- JEONG, J. & HUSSAIN, F. 1995 On the identification of a vortex. *J. Fluid Mech.* **285**, 69–94.
- KRAVCHENKO, A. G. & MOIN, P. 1998 B-spline methods and zonal grids for numerical simulations of turbulent flows. *Report No. TF-73*. Department of Mechanical Engineering, Stanford University
- LILLY, D. K. 1992 A proposed modification of the Germano subgrid scale closure method. *Phys. Fluids*, **4**, 633–635.
- MITTAL, R. & MOIN, P. 1997 Suitability of upwind-based finite difference schemes for large-eddy simulation of turbulent flows. *AIAA J.* **35**, 1415–1417.
- NORBERG, C. 1987 Effect of Reynolds number and a low-intensity freestream turbulence on the flow around a circular cylinder. *Publ. 87/2* Dept. Applied Thermodynamics and Fluid Mechanics, Chalmers University of Technology
- PRASAD, A. & WILLIAMSON, C. H. K. 1996 The instability of the separated shear layer from a bluff body. *Phys. Fluids*, **8**, 1347–1349.
- PRASAD, A. & WILLIAMSON, C. H. K. 1997 The instability of the shear layer separating from a bluff body. *J. Fluid Mech.* **333**, 375–402.
- UNAL, M. F. & ROCKWELL, D. 1988a On vortex shedding from a cylinder: Part 1. The initial instability. *J. Fluid Mech.* **174**, 491–512.
- WEI, T. & SMITH, C. R. 1986 Secondary vortices in the wake of a circular cylinder. *J. Fluid Mech.* **169**, 513–533.